

†Professor, School of Engineering Science and Mechanics.  
Associate Fellow AIAA.

investigation are presented both in graphic and tabular form for several examples.

## II. Mathematical Formulation

Given an imperfect ( $w^0$ ), stiffened, thin, circular cylindrical shell of finite length  $L$  and various boundary conditions under the application of axial compression, lateral pressure, and torsion, the equilibrium equations can be derived by employing the steps outlined in Ref. 1. By introducing the Airy stress function as

$$\begin{aligned} N_{xx} &= -\bar{N}_{xx} + F_{,yy} \\ N_{yy} &= F_{,xx} \\ N_{xy} &= \bar{N}_{xy} - F_{,xy} \end{aligned} \quad (1)$$

where  $\bar{N}_{xx}$  is the applied uniform compression and  $\bar{N}_{xy}$  is the applied torsional stress resultant, the equilibrium and compatibility equations in terms of  $w$  and  $F$  become

$$\begin{aligned} DL_h[w] - Lq[F] - \frac{F_{,yy}}{R} - L[F, w + w^0] + \bar{N}_{xx}(w_{,xx} \\ + w^0_{,xx}) - 2\bar{N}_{xy}(w_{,xy} + w^0_{,xy}) - p = 0 \end{aligned} \quad (2)$$

$$L_d[F] + L_q[w] + \frac{1}{2}L[w, w + 2w^0] + \frac{w_{,xx}}{R} = 0 \quad (3)$$

where the operators  $L_h$ ,  $L_q$ , and  $L_d$  are defined in Ref. 1, and  $p$  is the applied pressure.

The expression for the total potential is given by

$$\begin{aligned} U_T = \frac{1}{2E_{xxp}} \int_A [\beta_1 F_{,yy}^2 + \beta_2 F_{,xx}^2 + \beta_3 F_{,xx} F_{,yy} \\ + \beta_4 F_{,xy}^2] dA + \frac{D}{2} \int_A [\alpha_1 w^2_{,yy} + \alpha_2 w^2_{,xx} \\ + \alpha_3 w_{,xx} w_{,yy} + \alpha_4 w^2_{,xy}] dA - \frac{\bar{N}_{xx}}{2E_{xxp}} \int_A [2\beta_1 F_{,yy} \\ + \beta_3 F_{,xx}] dA - \frac{\bar{N}_{xy}}{2E_{xxp}} \int_A 2\beta_4 F_{,xy} dA - \int_A p w dA \\ + \frac{\pi RL}{E_{xxp}} (\beta_1 \bar{N}_{xx}^2 + \beta_4 \bar{N}_{xy}^2) - 2\pi RL (e_{AV} \bar{N}_{xx} + \gamma_{AV} \bar{N}_{xy}) \end{aligned} \quad (4)$$

where the coefficients  $\alpha_i$  and  $\beta_i$  are defined in Ref. 1, and the symbols  $e_{AV}$  and  $\gamma_{AV}$  denote the average end shortening and average shear strain, respectively. The mathematical expressions for these quantities are given by

$$\begin{aligned} e_{AV} = a_1 \bar{N}_{xx} - \frac{1}{2\pi RL} \int_0^{2\pi R} \int_0^L [a_1 F_{,yy} + a_2 F_{,xx} \\ + a_3 w_{,xx} + a_4 w_{,yy} - \frac{1}{2} w_{,x} (w_{,x} + 2w^0_{,x})] dx dy \end{aligned} \quad (5)$$

$$\begin{aligned} \gamma_{AV} = \frac{2\bar{N}_{xy}}{(1-\nu)E_{xxp}} - \frac{1}{2\pi RL} \int_0^{2\pi R} \int_0^L \left[ \frac{2F_{,xy}}{(1-\nu)E_{xxp}} \right. \\ \left. + w_{,x} w_{,y} + w_{,y} w^0_{,x} + w_{,x} w^0_{,y} \right] dx dy \end{aligned} \quad (6)$$

Similarly, the expressions for the end shortening and shear strain at  $y=0$  are given by

$$\begin{aligned} e(y=0) = a_1 \bar{N}_{xx} - \frac{1}{L} \int_0^L [a_1 F_{,yy} + a_2 F_{,xx} + a_3 w_{,xx} \\ + a_4 w_{,yy} - \frac{1}{2} w_{,x} (w_{,x} + 2w^0_{,x})]_{y=0} dx \end{aligned} \quad (5a)$$

$$\begin{aligned} \gamma(y=0) = \frac{2\bar{N}_{xy}}{(1-\nu)E_{xxp}} - \frac{1}{L} \int_0^L \left[ \frac{2F_{,xy}}{(1-\nu)E_{xxp}} \right. \\ \left. + w_{,x} w_{,y} + w^0_{,x} w_{,y} + w_{,x} w^0_{,y} \right]_{y=0} dx \end{aligned} \quad (6a)$$

The boundary conditions are developed in a manner similar to Ref. 1, and the general computer program is written to accommodate any combination of transverse and in-plane boundary conditions ( $SS_i, CC_i, FF_i, i=1,2,3,4$ )

$$\begin{array}{ll} SS & w = M_{xx} = 0 \\ CC & w = w_{,x} = 0 \\ FF & Q_x^* = M_{xx} = 0 \end{array} \quad \begin{array}{ll} 1) & F_{,xy} = F_{,yy} = 0 \\ 2) & F_{,xy} = 0 \quad u = C \\ 3) & v = C \quad F_{,yy} = 0 \\ 4) & v = C \quad u = C \end{array} \quad (7)$$

where  $C$  is a constant, and the conditions in  $u$  and  $v$  may be expressed in terms of  $w$  and  $F$  as in Ref. 9.

The first step in the methodology, employed herein as well as in Ref. 1, is to reduce the governing equations (2) and (3) from a system of coupled nonlinear partial differential equations to a system of coupled nonlinear ordinary differential equations. This is accomplished by employing the following separated form for  $w$  and  $F$ .

$$\begin{aligned} w(x,y) &= \sum_{i=0}^K \left[ A_i(x) \cos \frac{iny}{R} + B_i(x) \sin \frac{iny}{R} \right] \\ F(x,y) &= \sum_{i=0}^{2K} \left[ C_i(x) \cos \frac{iny}{R} + D_i(x) \sin \frac{iny}{R} \right] \end{aligned} \quad (8)$$

In addition, if one considers the imperfection to be, in general, asymmetric and the applied pressure position dependent, then similar expressions may be employed for  $w^0(x,y)$  and  $p(x,y)$ ,

$$\begin{aligned} w^0(x,y) &= \sum_{i=0}^K \left[ A_i^0(x) \cos \frac{iny}{R} + B_i^0(x) \sin \frac{iny}{R} \right] \\ p(x,y) &= \sum_{i=0}^K \left[ p_i^1(x) \cos \frac{iny}{R} + p_i^2(x) \sin \frac{iny}{R} \right] \end{aligned} \quad (9)$$

The reduction to ordinary differential equations is accomplished through the following steps.

1) Equations (8) and (9) are substituted into the compatibility equation (3). Then, by employing trigonometric identities involving products and the linear independence of the sine and cosine terms,  $(4K+1)$  coupled nonlinear ordinary differential equations are obtained. This substitution clearly shows why the summation in the  $F(x,y)$  expression is from zero to  $2K$ . These equations, which relate the  $A_i(x)$ ,  $B_i(x)$ ,  $C_i(x)$ , etc., are given as Eqs. (11) and (12) in Ref. 8, which is an expanded version of the present paper.

2) Equations (8) and (9) are substituted into the equilibrium equations (2), and the error is made orthogonal to  $\cos(iny/R)$  and  $\sin(iny/R)$  for  $i=0,1,2,\dots,K$ . This is a Galerkin-type procedure with respect to the circumferential direction. The vanishing of the  $(2k+1)$  Galerkin integrals leads to a system of  $(2k+1)$  nonlinear ordinary differential equations (equilibrium). These equations may also be found in Ref. 8, as Eqs. (14-16).

Note that the equations governing the response of the imperfect configuration to any level of the applied loading ( $\bar{N}_{xx}$ ,  $\bar{N}_{xy}$ ,  $p_i^1$ , and  $p_i^2$ ) for a given shape and magnitude of the imperfection ( $A_i^0$ ,  $B_i^0$ ) are reduced to a system of  $(6k+2)$  equations, in  $(6k+2)$  unknowns,  $A_i$  ( $i=0,1,\dots,K$ ),  $B_i$  ( $i=1,2,\dots,K$ ),  $C_i$  ( $i=0,1,\dots,2K$ ), and  $D_i$  ( $i=1,2,\dots,K$ ). Note that  $C_0$ , through Eq. (1), has been eliminated from the remaining equations. In these governing equations, one more undetermined parameter is present, the wave number  $n$ . This

number is established by requiring the total potential to be a minimum at the equilibrium point (see Refs. 1 and 8). Because of this, the expression for the total potential is needed, which is also given in Ref. 8, as well as the expressions for the average unit end shortening  $e_{av}$  and unit end twist  $\gamma_{av}$ . In addition, the expressions for the average unit end shortening and unit end twist at  $y=0$  are given in Ref. 8. These parameters are used as characteristic displacement or rotation in characterizing equilibrium states (load-deflection curves). The reason for their use instead of that of the average values is because the resulting plots are better and more distinguishable.

Finally, the appropriate boundary conditions are also expressed in terms of  $A_i$ ,  $B_i$ ,  $C_i$ , and  $D_i$ .

### III. Solution Procedure

The solution procedure employed herein is a modification of the procedure described in Ref. 1. A generalization of Newton's method, applicable to differential equations, serves to reduce the nonlinear field equations, and the appropriate boundary conditions to a sequence of linear systems. In this method, the iteration equations are derived by assuming that the solution is achieved by a small correction to an approximate solution (initially taken as the linear solution). These small corrections are obtained from the solution of the linearized (with respect to the corrections) differential equations. The ordinary differential equations are cast into the form of finite difference equations as in Ref. 1. The unknown vector  $Z$  contains  $(12K+2)$  elements

$$\{Z\}^T = \{A_0, A_1 \dots A_K, B_1 \dots B_K, C_1 \dots C_{2K}, D_1 \dots D_{2K},$$

$$A''_0, A''_1 \dots A''_K, B''_1 \dots B''_K, C''_1 \dots C''_{2K}, D''_1 \dots D''_{2K}\}$$

Note that the second derivatives (of  $A_i$ ,  $B_i$ ,  $C_i$  and  $D_i$ ) are considered as independent elements of the vector  $\{Z\}$ .

By using one fictitious point on each exterior side of the cylinder ends, one can write a system of  $(12K+2)(NP+2)$  difference equations, where  $NP$  denotes the number of mesh points. This system of difference equations can be solved by the special algorithm reported in Ref. 10 when a unique solution exists for a given set of applied loads. When the set of applied loads corresponds to a critical condition (limit point), a unique solution does not exist and thus the solution of the system of difference equations fails to converge. On the basis of these observations, the description of the solution procedure is as follows: First, the system of difference equations is solved for a small level of the applied load. Then, a multiple of this solution is used for a small increase in the load parameter. At each step, the value of  $n$  is needed to accomplish a solution. To this end, different values of  $n$  are used to obtain a solution. The solution that corresponds to the value of  $n$  that minimizes the total potential is considered as the correct one for that step. Numerical integration is used to find the total potential. The number of  $n$  values needed to be tried at each step is small, since the circumferential mode does not vary significantly with small increases in the applied load. For the purpose of minimizing the time required to accomplish a solution, judgment, based on experience, is used, which provides a balance between load step size (and consequently number of steps) and number of  $n$  values at each step. Numerical integration is also used, at each step, to compute the corresponding unit end shortening and/or average shear strain. Finally, this procedure is continued until the solution of the system of difference equations fails to converge. The associated load level corresponds to the critical condition.

In the case of combined loads, the procedure is virtually the same, but only one of the loads is increased while the remaining are kept constant. The ones kept constant are those that are small by comparison to the linear theory individual load application critical condition. For example, consider the

case of a configuration under the application of uniform axial compression  $\bar{N}_{xx}$  and torsion  $\bar{N}_{xy}$ . For this case, suppose that one is interested in finding the effect that a given imperfection has on the critical condition (this means to find the critical curve in the  $\bar{N}_{xx}$ ,  $\bar{N}_{xy}$  space that corresponds to this imperfection, and compare it to the critical curve that corresponds to perfect geometry and is obtained through linear theory). Through the use of linear theory the critical curve can be found for a given structural configuration (see Fig. 1). The intercepts denote critical loads under individual application (from the typical curve of Fig. 1 these values are  $\bar{N}_{xx_{crL}} = 5\bar{A}$  and  $\bar{N}_{xy_{crL}} = 8\bar{A}$  where  $\bar{A}$  is some numerical constant). From the nonlinear procedure, outlined herein for individual load application and a given imperfection, one can find the nonlinear theory critical loads (see Fig. 1,  $\bar{N}_{xx_{crNL}} = 3\bar{A}$ , and  $\bar{N}_{xy_{crNL}} = 7\bar{A}$ ). To find the complete curve one can 1) fix  $\bar{N}_{xy} = \bar{A}$  and  $2\bar{A}$  and employ the methodology by increasing  $\bar{N}_{xx}$  to find points I and II and 2) fix  $\bar{N}_{xx} = \bar{A}$  and increase  $\bar{N}_{xy}$  to find point III.

There is an alternate approach in constructing the nonlinear critical curve. This approach requires that both  $\bar{N}_{xx}$  and  $\bar{N}_{xy}$  be increased linearly (along line  $OP$  corresponding to some angle  $\theta$ ) to find the critical combination, point III, for that  $\theta$  value. Then vary  $\theta$  from zero to  $\pi/2$  and the complete curve is generated. Both approaches are incorporated into the computer program.

Regardless of the approach used, the ratio  $|\overline{OIII}|/|\overline{OP}|$  is a measure of the imperfection sensitivity (instead of  $|\overline{QIII}|/|\overline{QP'}|$ ). This ratio may be called knockdown factor and denoted by  $\Lambda$ .

### IV. Numeric Results and Discussion

The present methodology is demonstrated through a number of illustrative examples. Numerical solutions are obtained by employing the Georgia Tech high-speed digital computer CDC-CYBER 70, Model 74-28.

A general computer program is written that includes the following features: 1) It is applicable to a stiffened configuration, in either or both directions, as well as to an unstiffened configuration. 2) It accommodates all possible boundary conditions ( $SSi$ ,  $CCi$ ,  $FFi$ , etc.), and it can easily be modified to accommodate elastic end restraints. 3) The number of Fourier terms  $K$  can be as large as needed for accuracy. The same is true for the number of mesh points  $NP$  in the finite difference scheme. 4) The shape of the geometric imperfection is unrestricted. 5) It is applicable to any individual or combined application of uniform axial compression, torsion, and space-dependent lateral pressure. 6) The CPU time required to obtain a solution is reasonably small. For example, by using  $K=1$  and  $NP=57$  (826 unknowns) a solution (critical load and all intermediate steps) is obtained in 18 sec. For low load levels, a convergent solution is obtained through two iterations. For load levels approaching the limit point a convergent solution is obtained through six iterations. The solution has converged if the percent difference in response between two consecutive iterations is smaller than  $10^{-4}$ .

The numerical results for all illustrative examples (10) are presented in Table 1. The geometric parameters and load conditions for each example number are shown. In addition, the perfect geometry (linear theory) results, the imperfection analysis results (present nonlinear theory), and the associated knockdown factor,  $\Lambda$ , are shown. For all 10 examples the boundary conditions are taken to be classical simply supported ( $SS3$ ). Poisson's ratio for examples 4 and 5 is 0.3333, whereas for the remaining examples it is 0.3.

Examples 1, 2, and 3 have been reported in Refs. 1 and 7. The imperfection considered, for these examples, herein is

$$w^0(x, y) = t \sin \frac{m\pi x}{L} \left( \cos \frac{ny}{R} + \sin \frac{ny}{R} \right)$$

Table 1 Final results for imperfect stiffened cylindrical shell

Example no.	$E = (10.5)10^6$ Geom. etric parameters										Loading	Linear buckling load, perfect cylinder				Imperfection amplitude $\delta/t$	Nonlinear solution, imperfect cylinder				
	$L$	$R$	$t$	$Z$	$\frac{e_x}{t}$	$\frac{e_y}{t}$	$\bar{N}_{xx}$	$\bar{N}_{yy}$	$\bar{p}_{xx}$	$\bar{p}_{yy}$		$\bar{N}_{xxcl}$	$\bar{N}_{xycl}$	$p_{cl}$	$n_{cl}$		$\bar{N}_{xxcr}$	$\bar{N}_{xycr}$	$p_{cr}$	$\Lambda$	$n_{cr}$
1	4	4	0.04	95.4	6	3	0.91	0.455	100	20	$\bar{N}_{xx}$	19,790	—	—	4	1.0	15,250 15,630	—	—	0.771-0.790	4
2	4	4	0.04	95.4	6	6	0.91	0.91	100	100	$p$	—	—	7060	4	1.0	—	—	6500	0.92	4
3	4	4	0.04	95.4	-6	-6	0.91	0.91	100	100	$\bar{N}_{xx} = \frac{pr}{2}, p$	16,200	—	8100	4	1.0	9385	—	4693	0.579	4
4	4	8	0.1886	10	0	0	0	0	0	0	$\bar{N}_{xy}$	—	30,660	—	8	1.0	—	16,500	—	0.538	8
5	16	4	0.006	10000	0	0	0	0	0	0	$\bar{N}_{xy}$	—	7.04	—	9	1.0	—	5.0	—	0.714	9
6	4	4	0.04	95.4	6	3	0.91	0.455	100	20	$\bar{N}_{xy}$	—	26,260	—	5	1.0	—	21,500	—	0.819	5
7	4	4	0.04	95.4	6	3	0.91	0.455	100	20	$\bar{N}_{xy}$	—	26,260	—	5	2.0	—	20,500	—	0.781	4
8	4	4	0.04	95.4	6	3	0.91	0.455	100	20	$\bar{N}_{xy}$	—	26,260	—	5	3.0	—	20,000	—	0.762	4
9	4	4	0.04	95.4	6	3	0.91	0.455	100	20	$\bar{N}_{xy}$	—	26,260	—	5	5.0	—	20,000	—	0.762	4
10	4	4	0.04	95.4	6	3	0.91	0.455	100	20	$\bar{N}_{xx} = 8000$	8000	20,280	—	4	1.0	8000	16,250	—	0.856	5

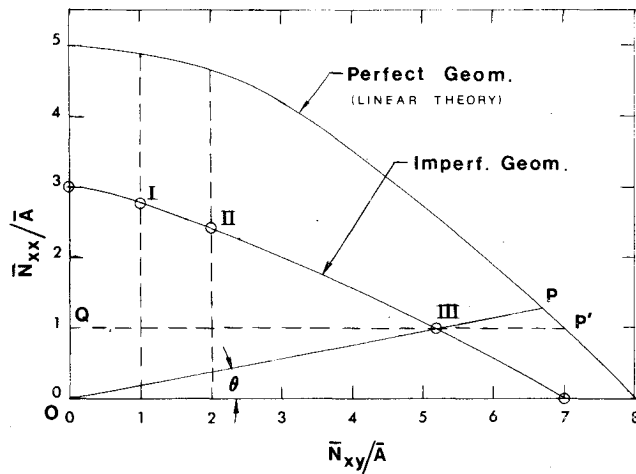


Fig. 1 Critical conditions under combined loads (typical qualitative curves).

Although a more general imperfection shape is used in this paper [in Refs. 1 and 7 the imperfection shape was taken to be symmetric,  $\cos(ny/R)$  only] the results are the same because, in the absence of torsion, there is no coupling between sine and cosine terms.

Examples 4 and 5 correspond to an unstiffened configuration under torsion only, and they correspond to cases that have been worked out previously (see Ref. 6) by employing a Koiter-type analysis. The difference between these examples is the curvature parameter ( $Z=10$  for example 4, and  $Z=10^4$  for example 5). A comparison between the present results and those of Ref. 6 shows very good agreement for both cases. The imperfection for these two examples was taken to be

$$w^0(x, y) = \delta \sum_{m=1}^s \left[ A_m \cos \frac{ny}{R} + B_m \sin \frac{ny}{R} \right] \sin \frac{m\pi x}{L} \quad (10)$$

with  $\delta=t$  and  $A_m$  and  $B_m$  are the elements of the corresponding perfect geometry linear theory eigenvector.

Note that in the case of torsion there are two different eigenvectors (linear theory), one corresponding to positive torsion and one to negative torsion. Since the imperfection shape is considered to be similar to this eigenvector, the analysis is performed to check the effect of one on the other.

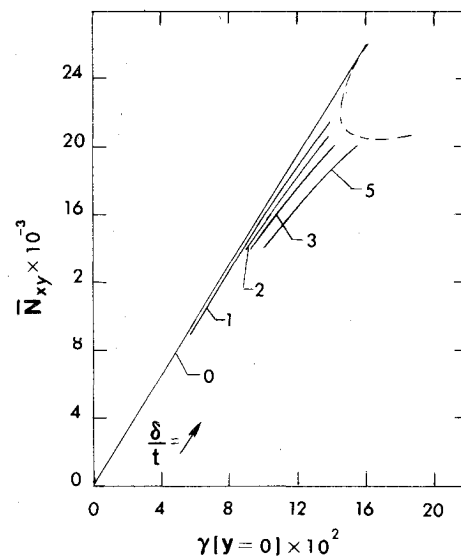


Fig. 2 Load vs angle of twist for imperfect stiffened cylinders (examples 6-9).

It is found that an imperfection shape similar to the positive torsion eigenvector has virtually no effect on the load carrying capacity when the torsion is applied in the negative direction. (The shell is insensitive and thus  $\Lambda=1$ .) This reinforces the contention that the shell is sensitive to imperfection shapes that are similar to the corresponding perfect geometry linear theory eigenvector. This observation is made for all other examples with torsional loads.

Examples 6 through 9 correspond to a stiffened configuration (same for all four), imperfection shapes characterized by Eq. (10), and different imperfection amplitudes ( $\delta=t, 2t, 3t$ , and  $5t$ , respectively). The results for these cases are also presented graphically on Figs. 2 and 3. Two observations are worth mentioning here. First, the "guessed" postbuckling behavior (see dotted line on Fig. 2) indicates that shells loaded in torsion are not as sensitive to geometric imperfections as those loaded in axial compression. This is in agreement with the qualitative results of Ref. 3. Second, stiffened configurations of the same curvature parameter (based on actual thickness) or a weighted curvature parameter (based on a weighted thickness that includes the smeared stiffener contribution) are not as sensitive as the corresponding unstiffened configurations. According to Ref. 6 (see Table 1; Case I and Fig. 6 of Ref. 6) the knockdown

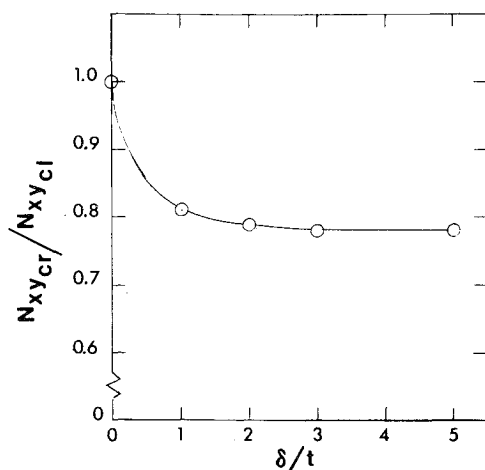


Fig. 3 Knockdown factor vs imperfection amplitude (examples 6-9).

factor for an unstiffened configuration with  $Z < 96$  is definitely smaller than 0.6 ( $\Lambda < 0.6$ ), while for these stiffened geometries  $\Lambda \geq 0.76$ .

Finally, example 10 corresponds to the same stiffened configuration as examples 1 and 6 through 9 but under combined application of axial compression and torsion. The imperfection shape for this example, also, is taken to be similar to the classical perfect geometry eigenvector. Since, for this geometry, the analysis is performed for individual load application (examples 1 and 6), the knockdown factor is computed as described in the previous section (see Fig. 1).

#### Acknowledgments

This work was sponsored by the Air Force Office of Scientific Research, Air Force Systems Command, USAF, under AFOSR Grant 74-2655. This support and the con-

tinuous encouragement by Mr. William Walker are gratefully acknowledged.

#### References

- <sup>1</sup>Sheinman, I. and Simites, G.J., "Buckling of Geometrically Imperfect Stiffened Cylinders under Axial Compression," *AIAA Journal*, Vol. 15, March 1977, pp. 374-382.
- <sup>2</sup>Loo, T.T., "Effects of Large Deflections and Imperfections on the Elastic Buckling of Cylinders under Torsion and Axial Compression," *Proceedings of the Second U.S. National Congress of Applied Mechanics*, 1954, pp. 345-375.
- <sup>3</sup>Nash, W.A., "Buckling of Initially Imperfect Cylindrical Shells Subjected to Torsion," *Journal of Applied Mechanics*, Vol. 24, 1957, pp. 125-130.
- <sup>4</sup>Koiter, W.T., "On the Stability of Elastic Equilibrium," in Dutch, Thesis, Delft, Amsterdam 1945; English Translation NASA TT-F-10833, 1967.
- <sup>5</sup>Koiter, W.T., "Elastic Stability and Post-Buckling Behavior," *Nonlinear Problems*, R.E. Langer, editor, University of Wisconsin Press, Madison, 1963, pp. 257-275.
- <sup>6</sup>Budiansky, B., "Post-Buckling Behavior of Cylinders in Torsion," *Theory of Thin Shells* (IUTAM Symposium, Copenhagen, 1967, F.I. Niordson, editor), Springer-Verlag, Berlin, 1969.
- <sup>7</sup>Simites, G.J. and Sheinman, I., "The Effect of Initial Imperfections on Optimal Stiffened Cylinders under Axial Compression," AFOSR TR-77-0639, Georgia Institute of Technology, Atlanta, Ga., March 1977.
- <sup>8</sup>Sheinman, I. and Simites, G.J., "Buckling of Imperfect Stiffened Cylinders under Destabilizing Loads Including Torsion," *Proceedings of AIAA/ASME 18th Structures, Structural Dynamics and Material Conference*, Vol. A, San Diego Calif., March 1977, pp. 260-269.
- <sup>9</sup>Narasimhan, K.Y. and Hoff, N.J., "Calculation of the Load Carrying Capacity of Initially Slightly Imperfect Thin Walled Circular Cylindrical Shells of Finite Length," *SUDAER No. 329*, Stanford University, Stanford, Calif., Dec. 1967.
- <sup>10</sup>Tene, Y., Epstein, M., and Sheinman, I., "A Generalization of Potter's Method," *Computers and Structures*, Vol. 4, 1974, pp. 1099-1103.

## Announcement: 1977 Author and Subject Index

The indexes of the five AIAA archive journals (*AIAA Journal*, *Journal of Aircraft*, *Journal of Energy*, *Journal of Hydronautics*, *Journal of Spacecraft and Rockets*) will be combined and mailed separately early in 1978. In addition, papers appearing in volumes of the *Progress in Astronautics and Aeronautics* book series published in 1977 will be included. Librarians will receive one copy of the index for each subscription which they have. Any AIAA member who subscribes to one or more Journals will receive one index. Additional copies may be purchased by anyone, at \$10 per copy, from the Circulation Department, AIAA, Room 730, 1290 Avenue of the Americas, New York, New York 10019. **Remittance must accompany the order.**

Ruth F. Bryans  
Director, Scientific Publications